INTERNATIONAL JOURNAL of RENEWABLE ENERGY RESEARCH
Z. Saberi et al., Vol.16, No.1, March, 2026

Electrical and Thermal Performance of an Integrated Bifacial Photovoltaic Thermal (bPVT) Collector Using Compound Parabolic Concentrator

Zainab Saberi*, Ahmad Fudholi**, ***‡, Mohammad Hafizuddin Hj. Jumali*, Hasila Jarimi**, Halim Hj. Razali**, Oo Abdul Rosyid***, Yadi Radiansah***, Dalmasius Ganjar Subagio***, Yusuf Suryo Utomo***, Kamaruzzaman Sopian****

* School of Applied Physics, Faculty of Science and Technology, National University of Malaysia, Malaysia

** Solar Energy Research Institute, National University of Malaysia, Malaysia

*** Research Center for Energy Conversion and Conservation, National Research and Innovation Agency (BRIN), Indonesia

**** Department of Mechanical Engineering, Universiti Teknologi PETRONAS, Seri Iskandar 32610, Perak, Malaysia

(zaii.saberi@gmail.com, ahmad.fudholi@brin.go.id, hafizhj@ukm.edu.my, hasila.jarimi@ukm.edu.my, drhalimrazali@ukm.edu.my, abdul65.rosyid@gmail.com, yadi003@brin.go.id, dalmasius@yahoo.com, yusu004@brin.go.id, ksopian@ukm.edu.my)

‡ Ahmad Fudholi, Solar Energy Research Institute, National University of Malaysia, Malaysia and Research Center for Energy Conversion and Conservation, National Research and Innovation Agency (BRIN), Indonesia, Tel: +6281275193956, ahmad.fudholi@brin.go.id

Received: 07.10.2023 Accepted:06.12.2023

Abstract- This study focused on bPVT collectors integrating CPC and mirrors as reflectors to capture radiation from both the front and rear sides, generating electricity and heat simultaneously. Experimental and analytical methods were used to assess the collector's performance, including electrical, thermal, and overall efficiency. Experimental validation of the bPVT system's thermal model showed partial agreement between theoretical and experimental results. The highest overall energy efficiency achieved was 74.65%, with a temperature output of 49.80 °C under a radiation intensity of 798.8 W/m² and an optimal mass flow rate of 0.0437 kg/s. Comparisons with prior research indicated the superiority of the integrated bPVT collector, achieving an efficiency of 84.61%, surpassing both monofacial and bifacial PVT air collectors. These findings advance bPVT collector technology, aiding in further design optimisation and integration into sustainable energy solutions.

Keywords Bifacial, CPC, photovoltaic, mirror, efficiency, mass flow rate.

Nomenclature

A	Surface area	Pr	Prandtl Number	θ	Accepetance half angle
C	Specific heat	Re	Reynolds number	σ	Stefan's Boltzman constant
CPC	Compound Parabolic Concentrator	$S_{1,\ldots,23}$	Factor used in matrices	Subscripts	
CR	Concentration Ratio	T	Temperature	r	Radiative
D_h	Hydraulic diameter	U_b	Top heat loss coefficient	a	Ambient
d	Channel depth	V	Wind velocity	b	Back plate
h	Heat transfer coefficient	W	Collector width	f	Fluid (air)
I	Solar irradiance	Greek Letters		g	Glass
k	Thermal conductivity	α	Absorptivity	i	Inlet
L	Length of the collector	τ	Transmitivity	o	Outlet
$\dot{m}$	Mass flow rate	μ	Viscocity	L	Laminate
Nu	Nusselt number	ρ	Reflectivity	m	Mirror
PF	Solar cell packing factor	ε	Emissivity	R	Reflector
		η	Efficiency	1 & 2	First and second channel

s Sky
t Insulation
w Wind

1. Introduction

Bifacial PVT, also known as Bifacial Photovoltaic Thermal systems, is an innovative technology that combines the benefits of both solar thermal technologies and solar photovoltaic (PV). It is an advanced form of solar energy system that can generate both electricity and heat from sunlight, making it a versatile and efficient solution for renewable energy production. The term "bifacial" refers to the ability of these systems to capture sunlight from both sides of the solar panels. In contrast to conventional PV systems, which harness only the sunlight directly striking the front side of the panels, bifacial PVT systems incorporate transparent or semi-transparent materials on the backside. This enables them to produce electricity from both direct sunlight and reflected sunlight from the ground or adjacent surfaces [1, 2]. This increases their overall energy output compared to conventional PV systems. Bifacial PVT systems are great because they can make electricity and heat at the same time, making the most of solar power [3, 4].

Bifacial PV panels can be used in solar power generation projects across Malaysia. Their ability to capture sunlight from both sides increases energy production and makes them suitable for various applications, including utility-scale solar farms, commercial rooftops and residential installations. Malaysia has vast water bodies, such as lakes, reservoirs, and dams. Bifacial PV panels can be employed in floating solar farms, where they can benefit from the reflection of sunlight off the water surface, enhancing energy generation [5]. In Malaysia's agricultural sector, bifacial PV panels can be utilised in agricultural greenhouses or shade structures, providing dual benefits of energy generation and shelter for crops [6]. This integration enables farmers to generate clean energy while optimising land use for agricultural purposes.

Bifacial PV panels can be incorporated into various public infrastructure projects in Malaysia, such as solar-powered bus stops, street lighting systems and carports. These installations can help reduce energy consumption from the grid and promote the use of sustainable energy sources. As a conclusion, the specific adoption and implementation of bifacial technology in Malaysia may differ depending on various factors, including government policies, market dynamics, and technological advancements [7].

Based on most research findings, PV monofacial panels have been predominantly used in the advancement of PVT collectors. In contrast to monofacial PV cells that absorb radiation from just one side, bPVT modules have the capacity to capture solar radiation from both sides, leading to increased electrical output. Additionally, the sturdier glass backing of bifacial PV cells contributes to their extended lifespan compared to monofacial PV cells [8]. Over the past few years, researchers have shown a significant increase in attention to bifacial PV panels, which has resulted in their extensive presence in the market, as depicted in Table 1.

By combining solar collectors and reflectors, it is possible to capture irradiation from a substantial reflective area. A solar collector receives this concentrated irradiance and utilises it to generate thermal energy at higher temperatures [13]. According to Lim et al. [14]; when combining a bifacial solar panel with a flat mirror positioned underneath, the total energy output is approximately 38.1% greater compared to a PV panel with black plywood on the back. Among the range of concentrating technologies, the Compound Parabolic Concentrator (CPC) stands out as the most widely adopted, thoroughly developed, and successfully implemented [15]. According to Damasen [16]; CPC has become the superior static low-concentration tool for photovoltaic applications over the past 20 years. This superiority stems from its enhanced optical efficiency and capability to capture both direct and diffuse sunlight [17]. This proficiency lies in its ability to efficiently redirect all incoming radiation, encompassing both direct and diffuse rays, towards a receiver, allowing for effective utilisation across a broad range of incidence angles.

Table 1. Research Findings on PV Panel Types and Energy Generation

Reference	Type of Panel	Energy Output Compared to Monofacial Panel
[9]	Bifacial PV and bPVT	Predicted market share to increase from 5% to 30% by 2027
[10]	Bifacial PV	Improvements ranging from 10 to 15%
[11]	Bifacial PV	Up to 30% more energy produced
[12]	Bifacial PV module in a PVT system	Approximately 40% more electrical energy generated than a monofacial PVT system

This investigation employs both mirrors and CPC technology. The mirror reflects the sunlight back towards the rear side of the bifacial PV solar cell, which is situated above the mirror and CPC arrangement. This study introduces a novel approach by investigating the performance enhancement possibilities of a double-pass configuration in a bifacial PVT air-based collector, incorporating CPC technology and a mirror reflector behind the bifacial PVT panel. The primary contributions of the paper encompass the design of a bifacial PVT solar collector integrating CPC with mirrors, theoretical evaluation using an energy balance-based mathematical model verified through experimentation, performance assessment of the newly designed collector through the established mathematical model, and the development of a comprehensive mathematical model derived from equations of energy balance. The study also emphasises the significance of conducting experimental work to validate the proposed theoretical model.

2. Methodology

In this study, a mathematical model for the bPVT) system is developed by utilizing an energy balance equation for each temperature node. The energy balance is established by evaluating the heat transfer mechanisms inherent in the bPVT solar collector. To illustrate the heat flow, a thermal nodal

network is employed, and Figure 1 depicts the schematic representation of this heat transfer process.

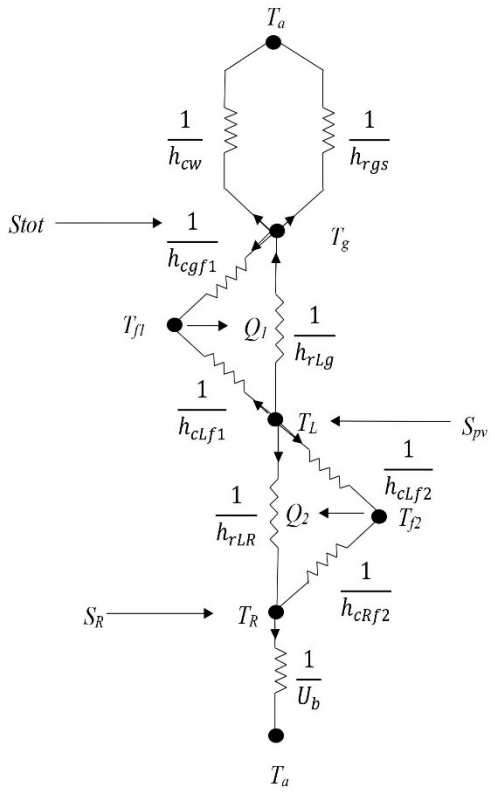

Fig.1. The thermal network for double pass bPVT collector.

2.1. Energy Balance Equation

The manuscript revolves around the central idea encapsulated in the main equations. These equations serve as the backbone of the proposed concept presented in the paper. According to the heat transfer analysis, the energy balance equations for each temperature node under steady-state conditions in the bPVT collector can be succinctly described as follows:

i. Glass cover

$$(h_{cw} + h_{rgs})(T_g - T_a) + h_{cgf1}(T_g - T_{f1}) = \alpha_g I + h_r L_g (T_L - T_g) \quad (1)$$

where T_g is the glass temperature, T_a is the ambient temperature, T_{f1} is the upper air flow temperature, T_L is the laminate temperature, α_g is the absorption of glass, and $h_r L_g$ is the radiative heat transfer from laminate to glass.

Part of the heat gain from sunlight at the glass is dissipated through:

a) Top loss ($Ut = h_{cw} + h_{rgs}$) to the ambient and sky.
b) Convective heat transfer to upper air flow (h_{cgf1}).

ii. Air flow in upper channel

$$Q_1 = h_{cgf1}(T_g - T_{f1}) + h_{cLf1}(T_L - T_{f1}) \quad (2)$$

where, Q_1 is the heat energy in upper channel, h_{cLf1} is the convective heat transfer from laminate to upper air flow.

Upper air flow gain heat from glass and bPV panel through convective heat transfer (h_{cgf1} and h_{cLf1}), then generate useful heat gain.

iii. PV Laminate

$$S_{pv} = h_{cLf1}(T_L - T_{f1})\left(\frac{A_L}{A_c}\right) + h_{cLf2}(T_L - T_{f2})\left(\frac{A_L}{A_c}\right) + h_{rLg}(T_L - T_g)\left(\frac{A_L}{A_c}\right) + h_{rLR}(T_L - T_R)\left(\frac{A_L}{A_c}\right) \quad (3)$$

where, $\left(\frac{A_L}{A_c}\right)$ is the area of laminate/area of collector; T_R is the reflector temperature; T_{f2}=Upper air flow temperature.

Part of the heat gain from sunlight at the PV panel (S_{pv}) is dissipated through:

a) Radiative heat transfer to glass and plate reflector (h_{rLg} and h_{rLR}).
b) Convective heat transfer to upper and lower air flow (h_{cLf1} and h_{cLf2}).

iv. Air flow in lower channel

$$Q_2 = h_{cLf2}(T_L - T_{f2})\left(\frac{A_L}{A_c}\right) + h_{cRf2}(T_R - T_{f2})\left(\frac{A_m}{A_c}\right) \quad (4)$$

where, $\left(\frac{A_m}{A_c}\right)$ is the area of mirror/area of collector.

Lower air flow gain heat from bPV panel and plate reflector through convective heat transfer (h_{cLf2} and h_{cRf2}), then generate useful heat gain.

v. Plate Reflector

$$S_R + \left(U_b\left(\frac{A_m}{A_c}\right)\right)T_a = -\left(h_{rLR}\left(\frac{A_L}{A_c}\right)\right)T_L - \left(h_{cRf2}\left(\frac{A_m}{A_c}\right)\right)T_{f2} + \left(h_{rLR}\left(\frac{A_L}{A_c}\right) + h_{cRf2}\left(\frac{A_m}{A_c}\right) + U_b\left(\frac{A_m}{A_c}\right)\right)T_R \quad (5)$$

where, U_b is the bottom loss to the ambient.

Part of the heat gain at the plate reflector (S_R) from the PV Laminate, CPC and mirror through radiation is dissipated through:

a) Bottom loss (U_b) from the backplate with insulation.
b) Convective heat transfer to lower air flow (h_{cRf2}).

where,

$$T_{f1} = \frac{(T_{f1,i} + T_{f1,o})}{2} \quad (6)$$

$$T_{f2} = \frac{(T_{f2,i} + T_{f2,o})}{2} \quad (7)$$

$$U_b = \frac{h_w . k_t}{h_w . t_t + k_t} \quad (8)$$

$$Q_1 = \frac{2\dot{m}C(T_{f1} - T_{f1,i})}{WL} \quad (9)$$

$$Q_2 = \frac{2\dot{m}C(T_{f2} - T_{f2,i})}{WL} \quad (10)$$

Taking into account the packing factors (PF) of the bifacial PV panel, S_R and Spv can be expressed as:

$$S_R(1-PF) = S_{total}\tau_g\tau_L\left[\left(\alpha_m\rho_R^{<\check{n}>}CR + \alpha_m\rho_L\rho_m\rho_R^{<2\check{n}>}\right)\right] \quad (11)$$

$$S_{pv} = S_{total}\tau_g\alpha_{pv}PF\left(1-\eta_{pvfront}\right) + S_{total}\tau_g\alpha_L(1-PF) + S_{total}(1-PF)\tau_g\tau_L\left[\rho_m\rho_R^{2\check{n}}\right]PF\alpha_{pv}CR\left(1-\eta_{pvrear}\right) + S_{total}(1-PF)\tau_g\tau_L\left[\rho_m\rho_R^{2\check{n}}\right](1-PF)\alpha_L CR \quad (12)$$

where, ň is an average number of reflections experienced by radiation that traverses a Compound Parabolic Concentrator (CPC) within the acceptance-half angle.

2.2. Simulation Procedure

In this study, the matrix solution method is employed to numerically solve the linear equations derived [18]. The set of equations, specifically Eq. (1) to (5), can be generally represented by a 5 x 5 matrix denoted as:

$$[A][T_{actual}] = [C] \quad (13)$$

The matrix [A], which has 5 rows and 5 columns, represents the matrix for the heat transfer coefficient. Similarly, the matrix [C] signifies the heat flux sources, while the matrix [T_{actual}] represents the temperatures to be calculated. Each of these letter matrices consists of 5 rows and 5 columns as in Eq. (14).

$$\begin{bmatrix} S_6 & S_7 & S_8 & 0 & 0 \\ S_9 & S_{10} & S_{11} & 0 & 0 \\ S_{12} & S_{13} & S_{14} & S_{15} & S_{16} \\ 0 & S_{17} & S_{18} & S_{19} & S_{20} \\ 0 & 0 & S_{21} & S_{22} & S_{23} \end{bmatrix} \begin{bmatrix} T_g \\ T_{f1} \\ T_L \\ T_{f2} \\ T_R \end{bmatrix} = \begin{bmatrix} S_1 \\ S_2 \\ S_3 \\ S_4 \\ S_5 \end{bmatrix} \quad (14)$$

where,

$$S_1 = \alpha_g I + (U_t)T_a \quad (15)$$

$$S_2 = -\left(\frac{2\dot{m}C}{WL}\right) T_{f1,i} \quad (16)$$

$$S_3 = S_{pv} \quad (17)$$

$$S_4 = \left(\frac{2\dot{m}C}{WL}\right) T_{f1,i} \quad (18)$$

$$S_5 = S_R + \left(U_b\left(\frac{A_m}{A_c}\right)\right) T_a \quad (19)$$

$$S_6 = h_{rLg} + h_{cgf1} + U_t \quad (20)$$

$$S_7 = -h_{cgf1} \quad (21)$$

$$S_8 = -h_{rLg} \quad (22)$$

$$S_9 = h_{cgf1} \quad (23)$$

$$S_{10} = -\left(h_{cgf1} + h_{cLf1} + \frac{2\dot{m}C}{WL}\right) \quad (24)$$

$$S_{11} = h_{cLf1} \quad (25)$$

$$S_{12} = -h_{rLg}\left(\frac{A_L}{A_c}\right) \quad (26)$$

$$S_{13} = -h_{cLf1}\left(\frac{A_L}{A_c}\right) \quad (27)$$

$$S_{14} = \left(h_{cLf1} + h_{cLf2} + h_{rLg} + h_{rLR}\right)\left(\frac{A_L}{A_c}\right) \quad (28)$$

$$S_{15} = -h_{cLf2}\left(\frac{A_L}{A_c}\right) \quad (29)$$

$$S_{16} = -h_{rLR}\left(\frac{A_L}{A_c}\right) \quad (30)$$

$$S_{17} = \frac{4\dot{m}C}{WL} \quad (31)$$

$$S_{18} = h_{cLf2}\left(\frac{A_L}{A_c}\right) \quad (32)$$

$$S_{19} = -\left(h_{cLf2}\left(\frac{A_L}{A_c}\right) + h_{cRf2}\left(\frac{A_m}{A_c}\right) + \frac{2\dot{m}C}{WL}\right) \quad (33)$$

$$S_{20} = h_{cRf2}\left(\frac{A_m}{A_c}\right) \quad (34)$$

$$S_{21} = -h_{rLR}\left(\frac{A_L}{A_c}\right) \quad (35)$$

$$S_{22} = -h_{cRf2}\left(\frac{A_m}{A_c}\right) \quad (36)$$

$$S_{23} = h_{rLR}\left(\frac{A_L}{A_c}\right) + h_{cRf2}\left(\frac{A_m}{A_c}\right) + U_b\left(\frac{A_m}{A_c}\right) \quad (37)$$

In this research study, the MATLAB software is employed to perform the iteration process utilizing the Newton-Raphson iteration technique for estimating the variables. A similar iterative modelling approach was utilized by Othman et al. [19]. The iteration process, depicted in detail in Figure 2, is necessary due to the temperature-dependent nature of the heat transfer coefficients.

2.3. Physical Properties

The collector's radiative and convective heat transfer coefficients is given by:

i. The coefficient for heat transfer h_w from the glass cover induced by wind is expressed as:

$$h_w = 5.7 + 3.8^*V_w \quad (38)$$

ii. The radiative heat transfer coefficient, h_rgs from the glass cover to the sky, as presented in [14]:

$$h_{rgs} = \frac{\sigma\varepsilon_g(T_g+T_s)(T_g^2+T_s^2)(T_g-T_s)}{T_g-T_a} \quad (39)$$

The temperature of the sky, Ts is determined by:

$$T_s = 0.0552\,T_a^{1.5} \quad (40)$$

iii. The radiative heat transfer coefficient, h_{rLg} from the laminate to the glass is given by:

$$h_{rLg} = \frac{\sigma(T_L+T_g)+(T_L^2+T_g^2)}{\left(\frac{1}{\varepsilon_{pv}}+\frac{A_L}{A_c}\right)+\left(\frac{1}{\varepsilon_g}-1\right)} \quad (41)$$

where,

$$A_c = W \text{ x } L \quad (42)$$

iv. The radiative heat transfer coefficient, h_{rLR} from the laminate to the reflector [20]:

$$h_{rLR} = \frac{\sigma(T_L+T_R)+(T_L^2+T_R^2)}{\frac{1}{\varepsilon_{pv}}+\frac{1}{\varepsilon_R}-1} \quad (43)$$

v. The convective heat transfer coefficient, h due to airflow in the channels:

$$h = \frac{k}{D_h} N_u \quad (44)$$

The hydraulic diameter D_h is determined by:

$$D_h = \frac{4Wd}{2(W+d)} \quad (45)$$

vi. The Prandtl number, Pr is calculated using the equation [21]:

$$Pr = \frac{\mu C}{k} \quad (46)$$

vii. The Reynolds number (Re), which determines the flow regime of a fluid, is given by [21]:

$$Re = \frac{\dot{m} D_h}{A_c \, x \, \mu} \quad (47)$$

viii. The Nusselt number, Nu is a dimensionless quantity that enhances the rate of heat transfer. It depends on the flow regime and is divided into the following three zones [22]:

a) Laminar flow regime, Re < 2300.

$$Nu = 5.4 + \frac{0.0190\left[Re\,(0.7)\left(\frac{D_h}{L}\right)\right]^{1.71}}{1+0.00563\left[Re\,(0.7)\left(\frac{D_h}{L}\right)\right]^{1.17}} \quad (48)$$

b) Transition flow regime, 2300 < Re < 6000.

$$Nu = 0.116\left(Re^{\frac{2}{3}} - 125\right) Pr^{\frac{1}{3}}\left[1 + \left(\frac{D_h}{L}\right)^{\frac{2}{3}}\right]\left[\frac{\mu}{\mu_w}\right]^{0.14} \quad (49)$$

c) Turbulent flow regime, Re > 6000.

$$Nu = 0.018 Re^{0.8} Pr^{0.4} \quad (50)$$

ix. According to Fudholi et al. [23], the subsequent equations determine these properties for air, the working fluid.

a. Air dynamic viscosity:

$$k = 0.02624 + 0.0000758(T - 27) \quad (51)$$

b. Density of air:

$$C = 1.0057 + 0.000066(T - 27) \quad (52)$$

c. Air thermal conductivity:

$$\mu = [1.983 + 0.00184\,(T - 27)] \text{ x } 0.00001 \quad (53)$$

d. Specific heat

$$\rho = 1.1774 - 0.00359(T - 27) \quad (54)$$

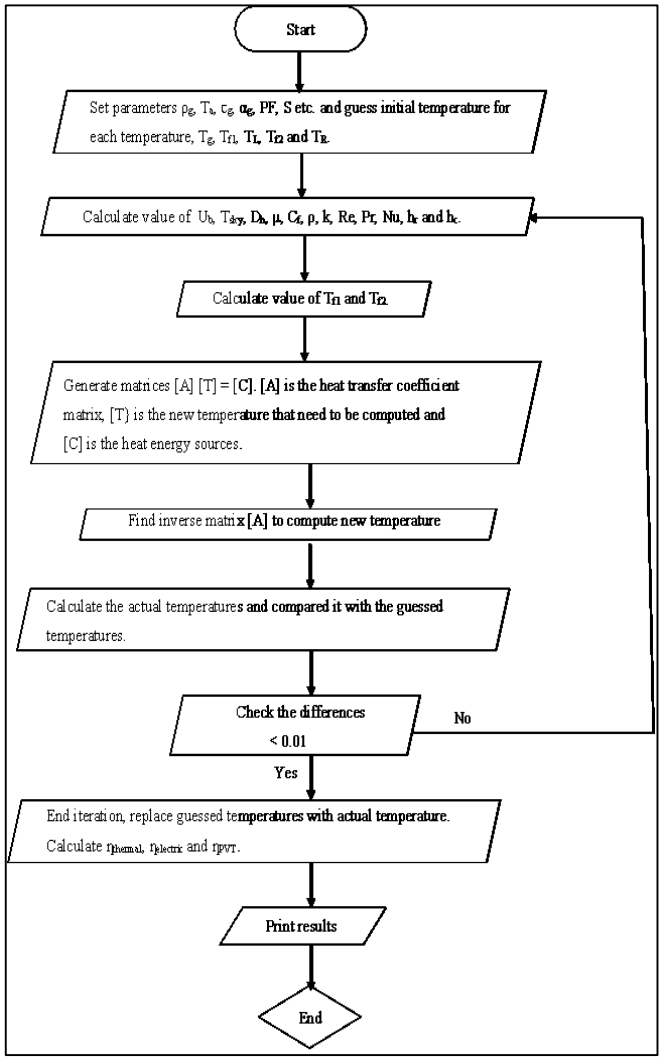

Fig. 2. Solution flow chart.

2.4. Performances Parameters

The electrical efficiency, denoted as η_{pv}, is affected by the solar cell's temperature and can be calculated using the following equation [24]:

$$\eta_{pv} = \eta_{ref}\left[1 - 0.005444\left(T_L - T_{ref}\right)\right] \quad (55)$$

To calculate the overall electrical efficiency, η_{pv} the electrical efficiencies of the front and back surfaces are added:

$$\eta_{pv} = \eta_{pvfront} + \eta_{pvrear} \quad (56)$$

Assuming that the electrical efficiency at the front and back surfaces is equal, we have:

$$\eta_{pvfront} = \eta_{pvrear} \quad (57)$$

Hence,

$$\eta_{pvfront} = \frac{1}{2}\eta_{pv} \quad (58)$$

The thermal energy efficiency of the solar collector is calculated using Eq. (59).

$$\eta = \frac{\dot{m}.(To-Ti).C}{A_C.I_C} \times 100\% \quad (59)$$

where ṁ, C, ΔT, Ac and I are the mass flow rate, specific heat capacity of the fluid, temperature difference, collector area, and solar irradiance, respectively. Therefore, the total energy efficiency of the PVT collector is the sum of thermal and electrical energy efficiency:

$$\eta_{PVT} = \eta_{pv} + \eta_{thermal} \quad (60)$$

To further validate the results, an accuracy calculation method commonly employed is used, as presented in Equation (61) [22]:

$$E = \frac{1}{n}\sum_{j=1}^{n}\frac{\left|\check{n}_{j-}n_j\right|}{\check{n}_j} \quad (61)$$

2.5 *Experimental Setup*

The design of appropriate collectors is a critical factor that impacts the performance of solar collectors. The bifacial solar panel is one of the main components in the PVT collector. In this study, the bifacial solar panel used exhibited a packing factor value of 0.5924. This particular panel comprises 36 bPV cells, as visually depicted in Figure 3.

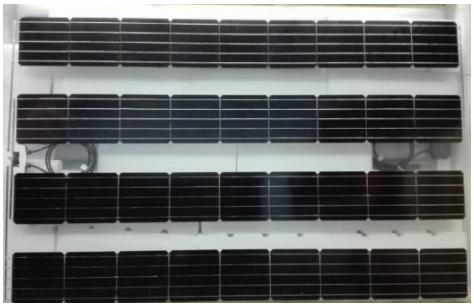

Fig. 3. Bifacial PV panel.

Figure 4 illustrates the design concept of the bPVT collector. The upper channel, comprised of the glass cover and the bifacial solar panel (bPV), permits air to enter and undergo direct heating from the solar simulator. The solar simulators emit light directed towards the front side of the bifacial PV module. Although some of the light is absorbed by the bifacial PV cells, the rest passes through the translucent section of the panel.

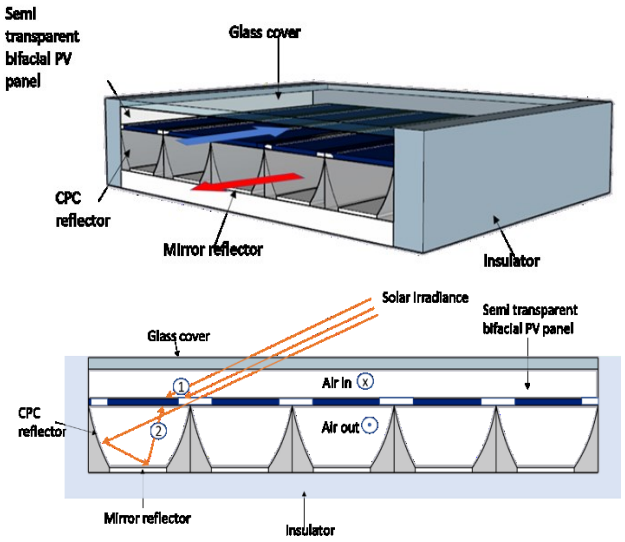

Fig. 4. The schematic model of a double pass double pass air-based bifacial PVT with CPC and mirror [25].

Subsequently, the heated air moves into the bottom channel, which is created by the bifacial solar panel and plate reflector (CPC and mirror). It then reaches the mirror and compound parabolic concentrator (CPC), which act as reflectors. From there, the light is reflected onto the back of the bifacial PV module. The presence of a CPC on the back of the photovoltaic panel enhances system effectiveness and facilitates heat transfer to the air.

In this study, plate reflectors are utilized to increases the intensity of radiation intensity on the receiver surface. This concentrated solar energy facilitates enhanced heat absorption by the receiver material, promoting higher thermal efficiency. Overall, the plate reflector holds a pivotal function in enhancing the gathering and application of solar energy within solar thermal systems. It guarantees proficient absorption of heat, reduces heat dissipation and adds to the comprehensive performance and efficiency of the system.

The carefully described experimental work approach is a key component of this paper and one of its main contributions, as validated by detailed experimental validation in Section 3.

3. Results and Discussion

3.1 *The influence of radiation intensity on the output power of the bPV panel*

The most commonly employed approach for assessing the effectiveness of a PV device involves examining its current and voltage characteristics through measurement. Figure 5 illustrates the current-voltage (I-V) curve for short-circuit current (I_{sc}) and open-circuit voltage (V_{oc}) obtained during each test conducted on a dual-sided PV panel under radiation intensities of 423.3 W/m², 501.4 W/m², 630.6 W/m² and 798.8 W/m². Additionally, Figure 6 demonstrates the power variations generated by the bPV cell within the same range of intensities.

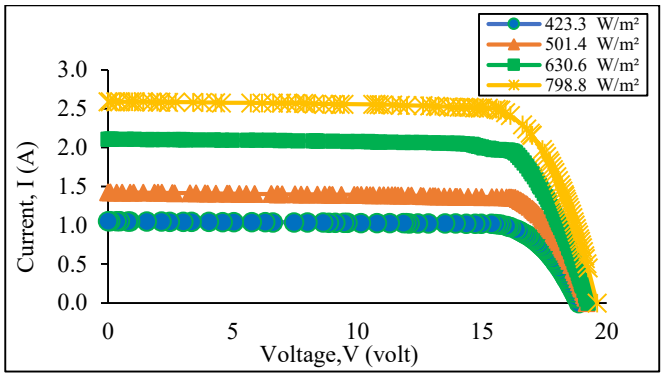

Fig. 5. I-V curve of bPV panel under varying radiation intensities

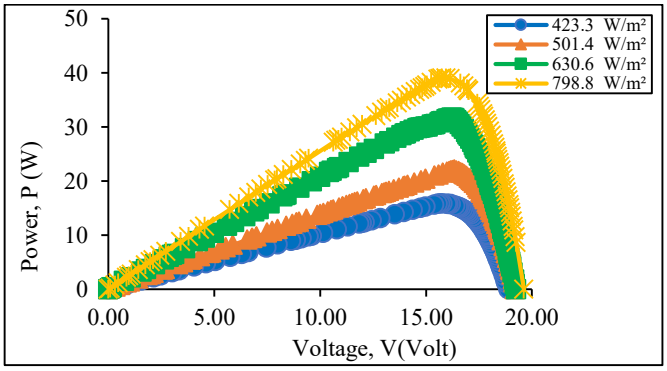

Fig. 6. The variation in power output of the bPV panel under different radiation intensities.

The details of the test results are provided in Table 2. At a constant panel temperature of 50°C, I_{sc} was found to increase with the received radiation intensity by the PV cell. I_{sc} changed from 1.055 A to 2.589 A as the radiation intensity shifted from 423.3 W/m² to 798.8 W/m². As the PV panel received higher radiation, an increased number of photon particles were absorbed. The energy from photons increased the flow of electrons, leading to a higher electric current. As a result, with higher radiation intensity, the bPV panel generates a greater power output. Furthermore, V_{oc} experienced a slight increase from 18.89 V to 19.62 V within the same intensity range.

Table 2. The electrical characteristics of bPV under varying radiation intensities

I (W/m²)	I_{sc} (A)	V_{oc} (V)	P_{max} (W)	Fill Factor (FF)
423.3	1.055	18.89	15.88	0.797
501.4	1.425	19.20	22.12	0.804
630.6	2.110	19.26	31.74	0.781
798.8	2.589	19.62	39.09	0.766

The fill factor (FF) declines from 0.797 at a radiation intensity of 423.3 W/m² to 0.766 when subjected to a radiation intensity of 798.8 W/m². FF is defined as the ratio of the maximum power (P_{max}) generated by the panel to the product of I_{sc} and V_{oc}. The decrease in FF is attributed to an increase in the internal resistance value, Rs, of the bPV panel as the radiation intensity increases [26].

Generally, the increase in I_{sc} is more pronounced compared to the slight increase in V_{oc} when the radiation intensity rises at a constant cell temperature. This condition allows P_{max} to increase from 15.88 W to 39.09 W when the radiation intensity changes from 423.3 W/m² to 798.8 W/m².

3.2 Impact of Air Mass Flow Rate on the Temperature of the bPV Panel and the Electrical Energy Efficiency of the PVT Collector

3.2.1. Temperature of the bPV panel

A mathematical model was developed to predict the thermal efficiency of a bPVT collector with CPC. The steady-state experimental results were contrasted with the projections of the mathematical model. The outcomes demonstrate that alterations in mass flow rates affect the temperature of a bPVT collector with CPC and thermal efficiency in distinct ways.

As depicted in Figure 7, elevating the mass flow rate leads to a simultaneous reduction in both the photovoltaic (T_{pv}) and output temperatures (T_o) of the bPVT collector with CPC at a radiation intensity of 798.8 W/m². This occurs because a larger volume of air is available to carry away heat from the channel walls, resulting in a lower PV temperature. The rate of heat transfer rises with higher air mass flow rates. Consequently, an increase in mass flow rate leads to a notable drop in the temperature of the photovoltaic panel (T_{pv}), particularly within the range of 0.0175 kg/s to 0.0437 kg/s. This, subsequently, results in cooler collector components and a decrease in the output air temperature.

At lower air mass flow rates, 0.0175 kg/s, the output temperature (T_o) is relatively high, measuring approximately 65.79°C (experiment) and 60.10°C (theory). However, as the mass flow rate is increased from 0.0175 kg/s to 0.0437 kg/s, the output temperature (T_o) experiences a significant decrease. Beyond a mass flow rate of 0.0437 kg/s, the reduction in output temperature (To) becomes smaller and remains nearly constant. These findings are consistent with the research conducted by other scholars [22].

In order to verify the accuracy of the mathematical model, a comparison was conducted between the model's predictions and the actual experimental findings. The mathematical model exhibited reasonably precise predictions, with an average error of 3.01% and 6.55% for outlet and PV temperature, respectively. Moreover, the results generated by the mathematical model closely matched the experimental data, achieving an accuracy rate of 97% for outlet temperature and 93.45% for PV temperature.

3.2.2. Temperature differences

The mass flow rate has an impact on the temperature rise within the collector, which represents the temperature difference between the output temperature (T_o) and the input temperature (T_i). Figure 8 illustrates the relationship between the temperature difference (ΔT, T_o- T_i) and the mass flow rate of air, as determined in the theoretical study. ΔT signifies the temperature difference between the incoming and outgoing air

within the solar collector, indicating the successful absorption and removal of heat by the air.

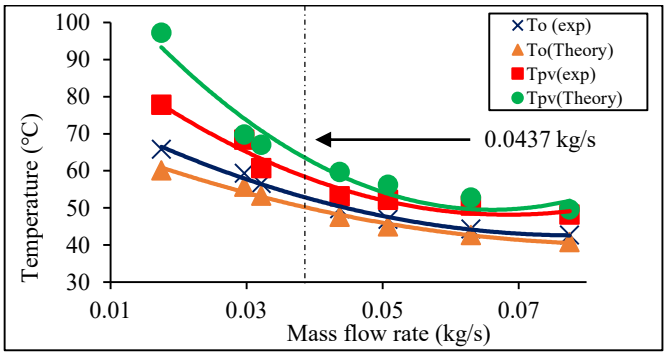

Fig. 7. Experimental and theoretical results of the PVT collector with CPC under radiation intensity of 798.8 W/m².

Under a radiation intensity of 501.4 W/m², the temperature rise decreases from 15.60°C to 6.32°C with an increase in air mass flow rate from 0.0175 kg/s to 0.0775 kg/s. This decrease in temperature rise is attributed to the heightened airflow entering the collector as the air mass flow rate rises [14]. However, this reduction in temperature increase does not follow a linear relationship with the increase in mass flow rate. Within the range of lower mass flow rates, from 0.0175 kg/s to 0.0437 kg/s, the temperature rise experiences a wider reduction. Conversely, for mass flow rates greater than 0.0437 kg/s, the reduction in temperature increase becomes smaller.

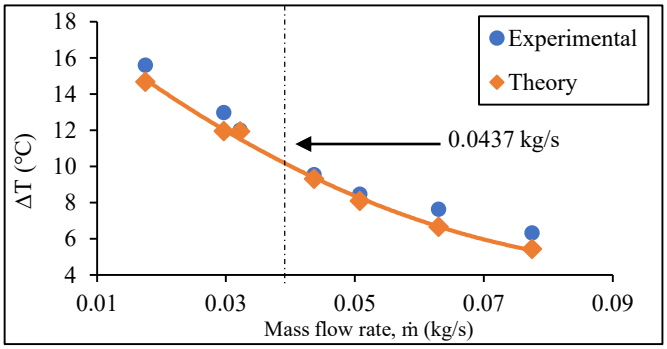

Fig. 8. Temperature difference versus mass flow rate at radiation intensity 501.4 W/m².

3.2.3. Energy efficiency

Figure 9 illustrate the energy efficiency of a BPVT collector with a CPC versus the mass flow rate, considering radiation intensities of 798.8 W/m². The PVT, electrical, and thermal efficiencies of the bPVT collector with a CPC exhibit an upward trend with increasing mass flow rate. Precisely, the collector's electrical efficiency rises with elevated mass flow rates across all levels of radiation intensity. This can be attributed to the faster cooling of photovoltaic cells at elevated air mass flow rates.

As depicted in Figure 9, the results show that the electrical efficiency decreases from 13.89% at a temperature of 48.19°C to 11.32% at a temperature of 77.86°C. This decrease in electrical efficiency results in an increase in the photovoltaic cell temperature, Tpv. The thermal efficiency of the collector undergoes changes when the mass flow rate varies from 0.0175 kg/s to 0.0775 kg/s. Figure 9 shows a change in thermal efficiency from 42.51% to 70.72%. However, the increase in efficiency is not linear with the increase in air mass flow rate across all radiation intensities. The most significant efficiency improvement occurs within the mass flow rate range of 0.0175 kg/s to 0.0437 kg/s, reaching an optimal efficiency value at mass flow rates greater than 0.0437 kg/s. This change in efficiency corresponds to the reduction in the collector's temperature rise resulting from increased mass flow rates.

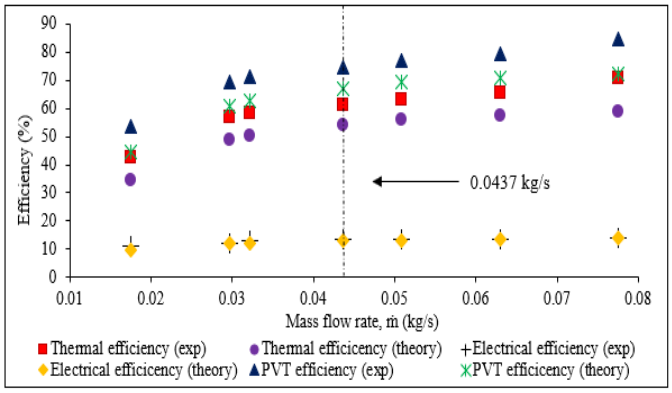

Fig. 9. Efficiency of energy as a function of mass flow rate at a radiation intensity of 798.8 W/m².

According to the experimental results, thermal efficiency and thermal efficiency increase with higher mass flow rates. Consequently, the combined efficiency, η_{PVT} of the collector also exhibits an upward trend as the air mass flow rate increases. Based on the graph above, the combined efficiency increases from 53.84% to 84.61%. The most significant increase occurs within the mass flow rate range of 0.0175 kg/s to 0.0437 kg/s, aligning with the increase in thermal efficiency. Beyond a mass flow rate of 0.0437 kg/s, the combined efficiency of the collector reaches its maximum value. As can see in Figure 9, the mathematical model exhibits a strong compatibility with the experimental data for PVT efficiency, achieving an accuracy of 91.22%. Similarly, the results for PV and thermal efficiencies indicate a high level of agreement between the mathematical model and experimental data, with accuracies of 96.85% and 89.56% respectively.

After analyzing the experimental data, it can be concluded that the efficiency of the collector, encompassing electrical, thermal, and combined aspects, is impacted by the flow rate of air in both the upper and lower channels. As the mass flow rate increases, there is a corresponding rise in the rate of heat transfer from the glass surface, panel surface, and reflector plate to the airflow. This results in a decrease in the output air temperature, as the heat from these surfaces is efficiently transferred, thereby keeping the collector cool. Consequently, the collector achieves its peak efficiency when the mass flow rate is elevated. The experimental results consistently demonstrate that the optimal efficiency of the collector is

achieved when the mass flow rate exceeds 0.0437 kg/s for all assessed radiation intensities.

Summary Table 3 provides a comprehensive overview of various studies conducted on monofacial and bifacial PVT air collectors for energy analysis. Remarkably, the present study showcases the highest total efficiency among previous research, reaching an impressive 84.61%. Consequently, the proposed design stands out as an exceptionally efficient solar collector, demonstrating its remarkable effectiveness in harnessing solar energy.

Table 3. Comparison of total efficiency from previous study

Ref.	Year	System design	Efficiency (%)		
			ηthermal	ηelectric	ηtotal
[27]	2017	Bifacial PVT with semi-mirror reflector	-	-	51-67
[28]	2018	Monofacial PVT with double pass using Fresnel lens and CPC	15-50	10-12.9	51-80
[29]	2019	Bifacial PVT collector	-	-	17-62
[18]	2020	Bifacial PVT collector with mirror reflector in a double pass configuration	24-47	5-9	20-57
[30]	2021	Bifacial PVT collector with cooling module	83.30	-	-
[31]	2021	Bifacial PVT with jet plate reflector	51.09	10.73	-
[32]	2021	Bifacial PVT system with glass channel	64.45	15.60	-
[8]	2022	Bifacial PVT with various cooling methods	35-57	12.70-14.20	-
[33]	2022	Bifacial PVT with jet impingement	57.30	10.36	83.93
Present study		Bifacial PVT with CPC and mirror reflector	70.72	13.89	84.61

4. Conclusion

In summary, this paper introduced a mathematical model for evaluating the performance of bPVT collectors equipped with CPC and mirrors, which was then compared to experimental findings. To solve the temperature equations for each element in the PVT system, a matrix inversion technique was employed. The results of the mathematical model, yielding an accuracy of about 96.85% for PV efficiency and 89.56% for thermal efficiency, demonstrated strong agreement with the experimental data. Across both theoretical and practical investigations, the average PVT energy efficiency achieved an accuracy of 91.22%. Based on this study, the following conclusions can be drawn:

(a) This paper introduces a novel design of a bifacial photovoltaic/thermal solar air collector with a CPC and a double pass mirror.

(b) The influence of radiation intensity on efficiency is minor, while the mass flow rate exerts a notable impact on efficiency.

(c) The highest thermal energy gain, electrical energy, and combined efficiency are achieved at a mass flow rate of 0.0775 kg/s, reaching 70.72%, 13.89%, and 84.61%, respectively.

(d) The collector's efficiency attains its optimum output at approximately 0.0437 kg/s mass flow rate. Beyond this point, further increases in mass flow rate yield only marginal gains in efficiency

Acknowledgements

The authors would like to thank the UKM for funding Geran Universiti Penyelidikan (GUP-2018-038), also the Solar Energy Research Institute (SERI), UKM for providing the laboratory facilities and technical support.

Author Contributions

Zainab Saberi: Original draft, conceptualization, methodology, visualization, validation. Ahmad Fudholi: Review and editing, methodology, investigation, validation, supervision. Mohammad Hafizuddin Hj. Jumali: Supervision. Hasila Jarimi: Formal analysis, review and editing; Halim Hj. Razali: Supervision. Oo Abdul Rosyid: methodology, formal analysis. Yadi Radiansah: Supervision, review and editing. Dalmasius Ganjar Subagio: Project administration. Yusuf Suryo: methodology, formal analysis. Kamaruzzaman Sopian: Project administration. All authors have read and agreed to the published version of the manuscript.

Conflict of Interest

The authors declare that they have no known competing financial interests or personal relationships that could have appeared to influence the work reported in this paper.

References

[1] A. Amjad, "Natural resources depletion, renewable energy consumption and environmental degradation: a comparative analysis of developed and developing world", International Journal of Energy Economics and Policy, vol. 11, pp. 251–260, February 2021.

[2] S. K. Sansaniwal, V. Sharma and J. Mathur, "Energy and exergy analyses of various typical solar energy applications: A comprehensive review", Renewable and Sustainable Energy Reviews, vol. 82, pp. 1576–1601, July 2018.

[3] Y. Jia, G. Alva, and G. Fang, "Development and applications of photovoltaic–thermal systems: A review", Renewable and Sustainable Energy Reviews, vol. 102, pp. 249–265, 2019.

[4] S. S. Joshi, and A. S. Dhoble, "Photovoltaic -Thermal systems (PVT): Technology review and future trends", Renewable and Sustainable Energy Reviews, vol. 92, pp. 848–882, April 2018.

[5] A. C Santos-Borja, "Dealing with uncertainties: Floating solar farm in natural lakes", IOP Conference Series: Earth and Environmental Science, vol. 789, pp. 012036, 2021.

[6] T. Sarker, M. Hussein, S. Mohammed, G. Ramasamy, F. Al Farid and S. Mansor, "Solar Photovoltaic Home Systems in Malaysia: A Comprehensive Review and Analysis", Energies MDPI, vol. 16, pp. 1–23. November 2023.

[7] H. Ziar, B. Prudon, F.Y. Lin, B. Roeffen, D. Heijkoop, T. Stark, S. Teurlincx, et al. "Innovative floating bifacial photovoltaic solutions for inland water areas. Progress in Photovoltaics", Research and Applications, vol. 29, pp. 725–743, October 2020.

[8] T. Ma, A. Kazemian, A. Habibollahzade, A. Salari, W. Gu, and J. Peng, "A comparative study on bifacial photovoltaic/thermal modules with various cooling methods", Energy Conversion and Management, vol. 263, pp. 115555, May 2022.

[9] W. Gu, T. Ma, M. Li., L. Shen, and Y. Zhang, "A coupled optical-electrical-thermal model of the bifacial photovoltaic module", Applied Energy, vol. 258, pp. 114075, October 2020.

[10] T. Katsaounis, K. Kotsovos, I. Gereige, A. Basaheeh, M. Abdullah, A. Khayat, E. Al-Habshi, et al., "Performance assessment of bifacial c-Si PV modules through device simulations and outdoor measurements", Renewable Energy, vol. 143, pp. 1285–1298, May 2019.

[11] U.A. Yusufoglu, T. H. Lee, T.M. Pletzer, A. Halm, L. J. Koduvelikulathu, C. Comparotto, R. Kopecek, et al., "Simulation of energy production by bifacial modules with revision of ground reflection", Energy Procedia, vol. 55, pp. 389–395, 2014.

[12] B. Robles-Ocampo, E. Ruíz-Vasquez, H. Canseco-Sánchez, R. C. Cornejo-Meza, G. Trápaga-Martínez, F. J. García-Rodriguez, J. González-Hernández, J., and Yu. V. Vorobiev, "Photovoltaic/thermal solar hybrid system with bifacial PV module and transparent plane collector", Solar Energy Materials and Solar Cells, vol. 91, pp. 1966–1971, 2007.

[13] D. Cabral, "Development and performance comparison of a modified glazed CPC hybrid solar collector coupled with a bifacial PVT receiver", Applied Energy, vol. 325, pp. 119653, June 2022.

[14] Y.S. Lim, C. K. Lo, S. Y. Kee, H. T. Ewe, H. T. and A. R. Faidz, "Design and evaluation of passive concentrator and reflector systems for bifacial solar panel on a highly cloudy region - A case study in Malaysia", Renewable Energy, vol. 63, pp. 415–425, 2014.

[15] O. Achkari, and A. El Fadar, "Latest developments on TES and CSP technologies – Energy and environmental issues, applications and research trends", Applied Thermal Engineering, vol. 167, pp. 114806, 2020.

[16] D. I. Paul, "Application of compound parabolic concentrators to solar photovoltaic conversion: A comprehensive review", International Journal of Energy Research, vol. 43, pp.1-48, January 2019.

[17] J. Akhter, S.I. Gilani, H.H. Al-kayiem, M. Ali and F. Masood, "Characterization and stability analysis of oil-based copper oxide nanofluids for medium temperature solar collectors", Mater. Werkst., vol. 50, pp. 311–319. 2019.

[18] M. Mustapha, A. Fudholi, and K. Sopian, "Mathematical modelling of bifacial photovoltaic-thermal (BPVT) collector with mirror reflector", International Journal of Renewable Energy Research, vol. 10, pp. 654–662, June 2020.

[19] M.Y.H. Othman, B. Yatim, K. Sopian, and M. N. Abu Bakar, "Performance analysis of a double-pass photovoltaic/thermal (PV/T) solar collector with CPC and fins", Renewable Energy, vol. 30, pp. 2005–2017, May 2005.

[20] M. M. Hegazy, A. El-Sebaii, M. R. Ramadan, S. Aboul-Enein, and A. E. M. Khallaf, "Comparative study of three different designs of a hybrid PV/T double-pass finned plate solar air heater", Environmental Science and Pollution Research, vol. 27, pp. 32270–32282, January 2020.

[21] N. S. Nazri, A. Fudholi, M. Hafidz Ruslan, and K. Sopian, "Mathematical Modeling of Photovoltaic Thermal-Thermoelectric (PVT-TE) Air Collector", International Journal of Power Electronics and Drive Systems (IJPEDS), vol. 9, pp. 795-802, June 2018.

[22] A. Fudholi, M. Zohri, G. L. Jin, A. Ibrahim, C.H. Yen, M. Y. Othman, M. H. Ruslan, and K. Sopian, "Energy and exergy analyses of photovoltaic thermal collector with ∇-groove", Solar Energy, vol. 159, pp. 742–750, 2018.

[23] A. Fudholi, M. Zohri, N. S. B. Rukman, N. S. Nazri, M. Mustapha, C.H. Yen, M. Mohammad and K, Sopian,

"Exergy and sustainability index of photovoltaic thermal (PVT) air collector: A theoretical and experimental study", Renewable and Sustainable Energy Reviews, vol. 100, pp. 44-51, 2019.

[24] M. Mustapha, A. Fudholi, C. H. Yen, M.H. Ruslan and K. Sopian, "Review on energy and exergy analysis of air and water based photovoltaic thermal (PVT) collector", International Journal of Power Electronics and Drive Systems, vol. 9, pp. 1367–1373, September 2018.

[25] Z. Saberi, H. Jarimi, M. H. Hj Jumali, S. Suhendri, S. Riffat, A. Fudholi, H. H. Razali and K. Sopian, "Performance assessment of double pass photovoltaic/thermal solar air collector using bifacial PV with CPC and mirror reflector under Malaysian climate", Case Studies in Thermal Engineering, vol. 44, pp. 102811, February 2023.

[26] A. D. Dhass, E. Natarajan and L. Ponnusamy, "Influence of shunt resistance on the performance of solar photovoltaic cell", International Conference on Emerging Trends in Electrical Engineering and Energy Management (ICETEEEM), Chennai, India, pp. 382-386, 2012.

[27] P. Ooshaksaraei, K. Sopian, S.H. Zaidi, and R. Zulkifli, "Performance of Four Air-Based Photovoltaic Thermal Collectors Configurations with Bifacial Solar Cells", Renewable Energy, 2017.

[28] B. S. S. Singh, C. H. Yen, S. H. Zaidi, and K. Sopian, "Part II: Enhanced performance of concentrating photovoltaic- thermal air collector with fresnel lens and compound parabolic concentrator (CPC)", Journal of Advanced Research in Fluid Mechanics and Thermal Sciences, vol. 47, pp. 16–24, July 2018.

[29] P. Ooshaksaraei, L. Ooshaksaraie, M. Seyednezhad, M. H. Yazdi, and K. Sopian, "Experimental and theoretical evaluation of bifacial photovoltaic thermal collectors", Computational Ecology and Software, vol. 9, pp. 121–133, December 2019.

[30] M. Hu, B. Zhao, X. Ao, Cao, J. Suhendri, Q. Wang, S. Riffat, Y. Su and G. Pei, "Performance analysis of a novel bifacial solar photothermic and radiative cooling module", Energy Conversion and Management, vol. 236, pp. 114057, March 2021.

[31] W. E. Ewe, A. Fudholi, K. Sopian and N. Asim, "Modelling of bifacial photovoltaic-thermal (PVT) air heater with jet plate", International Journal of Heat and Technology, vol. 39, pp. 1117–1122, 2021.

[32] H. Zhang, Y. Zhang, K. Liang, and H. Chen, "Performance study of a combined low-concentration bifacial photovoltaic/thermal system with glass channels", Renewable Energy, vol. 171, pp. 947–957. February 2021.

[33] W. E. Ewe, A. Fudholi, K. Sopian, R. Moshery, N. Asim, W. Nuriana, and A. Ibrahim, "Thermo-electro-hydraulic analysis of jet impingement bifacial photovoltaic thermal (JIBPVT) solar air collector", Energy, vol. 254, pp. 124366, May 2022.